First Experiments to Test Plasma Confinement by a Magnetic Dipole

J. Kesner 1), A.C. Boxer 1), J.L. Ellsworth 1), D. T. Garnier 2), A.K. Hansen 2), I. Karim 1), M. E. Mauel 2), E. E. Ortiz 2)

1) Plasma Science and Fusion Center, Massachusetts Institute of Technology, Cambridge, MA 02139, *USA*
2) Department of Applied Physics, Columbia University, New York, NY 10027, USA

e-mail address of main author: kesner@psfc.mit.edu

Abstract: We report the first production of high beta plasma confined by a laboratory superconducting dipole using neutral gas fueling and electron cyclotron resonance heating (ECRH). The pressure results from a population of anisotropic energetic trapped electrons that is sustained by microwave heating provided sufficient neutral gas is supplied to the plasma. The trapped electron beta was observed to be limited by the hot electron interchange (HEI) instability, but when the neutral gas was programmed so as to maintain the deuterium gas pressure near 0.2 mPa, the fast electron pressure increased by more than a factor of ten and the resulting stable high beta plasma was maintained quasi-continuously for up to 14 seconds. The levitated dipole experiment (LDX) is a new research facility that is investigating plasma confinement and stability in a dipole magnetic field configuration as a possible catalyzed DD fusion power source that would avoid the burning of tritium.

Introduction

The levitated dipole experiment (LDX), shown in Fig. 1, is a new research facility that is investigating the confinement and stability of plasma in a dipole magnetic field configuration [1]. We report the first production of high beta plasma confined by a laboratory dipole using neutral gas fueling and electron cyclotron resonance heating (ECRH) [2]. The pressure results from a population of energetic trapped electrons that is sustained for many seconds of microwave heating provided sufficient neutral gas is supplied to the plasma. In this case, the plasma stored energy was dominated by a population of anisotropic, $P_{\perp} > P_{\parallel}$, trapped energetic electrons with $E_{eh} > 50$ keV and $n_{eh} \sim 10^{17}$ m^{-3}.

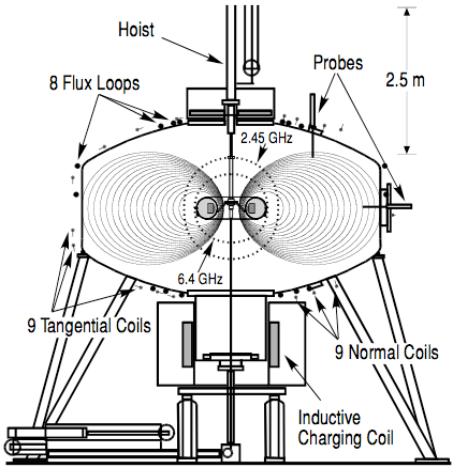

Fig. 1. Schematic of LDX device showing three superconducting magnets and the plasma configuration.

In the experiments reported here, high-beta plasma discharges were studied when the LDX high-field superconducting dipole magnet, termed the "floating coil" was supported by three thin support rods. In this mode of operation the main loss channel for both the hot and background species was loss to the supports. The equilibrium and stability properties are expected to be similar to those when the floating coil is magnetically levitated, whereas the transport is expected to improve substantially when the loss channel to the supports is removed. In this article we will discuss the equilibrium and stability properties of the LDX plasma when the floating coil is mechanically supported.

As shown in Fig. 1, LDX consists of an internal superconducting coil located within a 5 m diameter vacuum chamber. The coil's dipole moment is M = 0.34, I_d A-m^2, and experiments have been conducted with a dipole current up to I_d = 1.2 MA. A large bore superconducting coil, located below the main chamber, is used to inductively charge the dipole coil. The dipole is lifted for plasma experiments by a vacuum hoist. In this configuration three 1.5 cm diameter support rods intersect the plasma causing heat and particles to be lost from the plasma. In future experiments the coil will be magnetically levitated, eliminating losses to the support rods. Plasma diagnostics include 26 magnetic sensors to detect the plasma equilibrium current, probes to measure electrostatic fluctuations and edge plasma parameters, x-ray and visible light imaging cameras, and a microwave interferometer to measure the line-averaged plasma density.

The dipole confinement concept was motivated by spacecraft observations of planetary magnetospheres that show centrally-peaked plasma pressure profiles forming naturally when the solar wind drives plasma circulation and heating [3,4]. Unlike most other approaches to magnetic confinement in which stability requires average good curvature and magnetic shear, MHD stability in a dipole derives from plasma compressibility [5,6]. Dipole confinement is determined by the MHD prediction that a dipole-confined plasma remains stable below a critical pressure gradient [7]. At marginal stability $\delta(PV^\gamma) = 0$ (with P the plasma pressure, $V = \oint dl/B$ is the differential flux tube volume, and $\gamma = 5/3$), and an exchange of flux tubes does not modify the pressure profile. When flux tubes exchange adiabatically the plasma cools as it moves into lower fields and heats as it moves into higher fields and at marginality it remains in equilibrium with the local pressure as it circulates. Non-linear studies indicate that large-scale convective cells will form when the MHD stability limit is violated, which result in rapid circulation of plasma between the hot core and the cooler edge region [8]. Studies have also predicted that the confined plasma can be stable to low frequency (drift wave) modes and therefore we might expect that the energy confinement will remain close to the classical value. Additionally a levitated dipole device would be intrinsically steady state. Based on this model a properly designed dipole power source would ignite while maintaining MHD stability. For example, a dipole based power source using the catalyzed DD power cycle would eliminate the need for tritium breeding and for materials that maintain their integrity in a 14 MeV neutron irradiation environment [9].

3. High-β Equilibrium

Estimates of the plasma pressure are made by computing the least-squares best-fit of a model to the magnetic diagnostics. We use an anisotropic pressure profile, with $P_\perp > P_\parallel$, that is similar to that used to study plasma equilibrium and stability in the magnetic field of a point dipole [26, 27] and given by $P_\perp(\psi, B) = \hat{P}(\psi)(B_0(\psi)/B)^{2p}$ where $B = \nabla\phi \times \nabla\psi / 2\pi$ and $B_0(\psi)$ is the minimum field strength on a field-line. With this model, the ratio of perpendicular to parallel pressure is a constant, $P_\perp / P_\parallel = 1 + 2p$. To fit this model to the magnetic measurements, the plasma current, $J_\phi(r,z)$ is related to the pressure through the self-consistent equilibrium, $\psi(r,z)$. However, since the dipole moment of $J_\phi(r,z)$ is less than 2% of the coil's magnetic moment, the difference between $J_\phi(r,z)$ computed using the vacuum dipole field and the self-consistent field is undetectable for the beta achieved to date. Using the dipole's vacuum field, the plasma ring current density can be computed from any given function of $\hat{P}$ and parameter p using $J_\phi = -2\pi r[D_\psi P_\perp + 2pP_\perp D_\psi Ln(B)/(1+2p)]$ where $D_\psi \equiv |\nabla\psi|^{-2} \nabla\psi \cdot \nabla$. The detected signal from a magnetic sensor is computed by combining

contributions from $J_\phi(r,z)$ throughout the plasma with the decrease of I_d required to maintain constant the flux linked by the superconducting dipole. For the reconstructions reported here, $\hat{P}(\psi) = \Delta(\psi) \times P_0(\psi/\psi_0)^{4g}$, where $\Delta(\psi) = [(\psi - \psi_d)/(\psi_0 - \psi_d)]^\alpha$ is chosen to vanish at the surface of the dipole, ψ_d and to equal unity at the location of the pressure peak, ψ_0. Far from the coil's surface, $|\psi| << |\psi_d|$, the equatorial pressure is $P_\perp(r) \approx P_0(R_{peak}/r)^{4g}$. This form resembles the MHD condition for marginal stability, expressed as $\delta(PV^\gamma) = 0$ that is equal to $P \propto r^{4\gamma}$ in a dipole [5-7, 28].

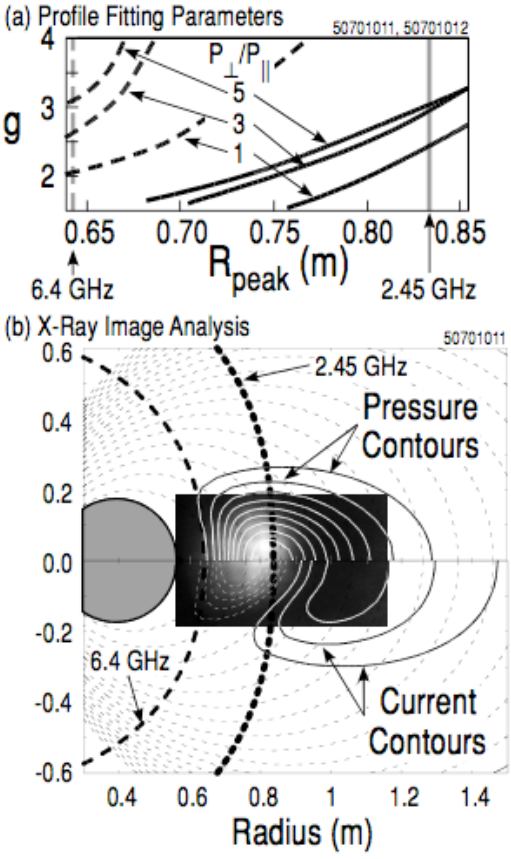

Fig.2 Profile parameters and contours of pressure and current that best fit magnetic measurements for discharges with single-frequency ECRH. X-ray image shows localization of fast-electrons.

Figure 2 illustrates the model pressure and current profiles that are the least-squares best fit to the magnetic measurements of high beta plasma produced with single-frequency ECRH. We find equally good fits occur either with steep profiles centered at large radii or with broad profiles centered at smaller radii. This results because J_ϕ is primarily determined from the pressure gradient and the magnetic sensors are most sensitive to the plasma's dipole moment. When only 2.45 GHz heating is applied (solid lines in Fig. 3a), very good fits result with $1.7 < g < 3.1$ when $0.68 < R_{peak} < 0.85$. Because we observe the fast-electron population to peak at the ECRH resonance, $R_{peak} = 0.83$ m, we conclude g = 2.0, 2.8, 3.1 for p = 0, 1, 2, respectively. When only 6.4 GHz microwaves are applied, $R_{peak} = 0.64$ m, and g = 2.0, 2.8, 3.5 for p= 0, 1, 2. Because of the dipole support rods, p > 0. From this, and previous experiments [14, 23] and the measured height of the x-ray images, we believe the pressure is well approximated by $P_\perp / P_\parallel \approx 5$. In future experiments additional diamagnetic loops will be located closer to the floating coil to permit a better resolution of the higher order moments of the current.

Figure 2b show the model $P_\perp$ and J_ϕ profiles that best fit measurements. Plasma with the highest values of I_p and β are created with both 2.45 GHz and 6.4 GHz heating. The sum of the mean-square deviations between the best-fit model profile and the magnetic measurements doubles as compared with single-frequency heating, and this may be related to the presence of two pressure peaks, one at each resonance. If R_{peak} is assumed to be midway between the resonances and p = 2, then 5 kW of heating creates a plasma (shot 50513029) with $I_p = 3.5$ kA, $\Delta I_f = -0.8$ kA, $W_p = 330$ J, g = 2.8, peak perpendicular pressure of 750 Pa, and maximum local beta of $\beta = (2\beta_\perp + \beta_\parallel)/3 = 21\%$. If R_{peak} moves outward closer to the 2.45 GHz resonance by 5 cm, β = 23%; moving inward by 4 cm towards the 6.4 GHz resonance, the best-fit results in β = 18%.

The radial location of the fast electron population is viewed by an x-ray camera during times when the ECRH is on as shown in Fig. 2b and by a visible camera that detects the ionization

glow of the trapped electrons after the microwave heating pulse ends. The x-ray camera contains a medical x-ray image intensifier sensitive to energies greater than 45 keV that was previously used during tokamak heating experiments [22]. A standard video camera is used to observe the fast electrons during the afterglow as described in Ref. [23]. For single frequency ECRH, the cameras indicate that the pressure peak is localized on the equatorial plane of the field lines having the fundamental cyclotron resonance at the minimum-B. This is expected for ECRH since the electrons that are mirror-trapped at the resonance are continuously heated by the injected microwaves [24, 25]. When both 2.45 GHz and 6.4 GHz sources are on, the x-ray image shows the fast electrons localized at the equator but span both resonances in the radial direction. Additional details and analyses of high beta dipole-confined plasma were presented in a longer article [28].

In the experiments reported here, the trapped electron beta was also limited by the low-frequency HEI discussed below, but when the neutral gas was programmed so as to maintain the deuterium gas pressure between about 1-3 μTorr, the fast electron pressure increased by more than a factor of ten and the stable high beta plasma could be maintained for many seconds. The high beta plasma generated a large equilibrium toroidal current, $I_p > 3$ kA, that is analogous to the ring current generated by high beta plasma in the Earth's magnetosphere [21]. Measurements of magnetic field of the plasma current and the location of fast electrons using x-ray imaging constrain models for the anisotropic pressure profile and allow estimates of the plasma stored energy, $W_p > 300$ J, and peak beta, $\beta \sim 20\%$.

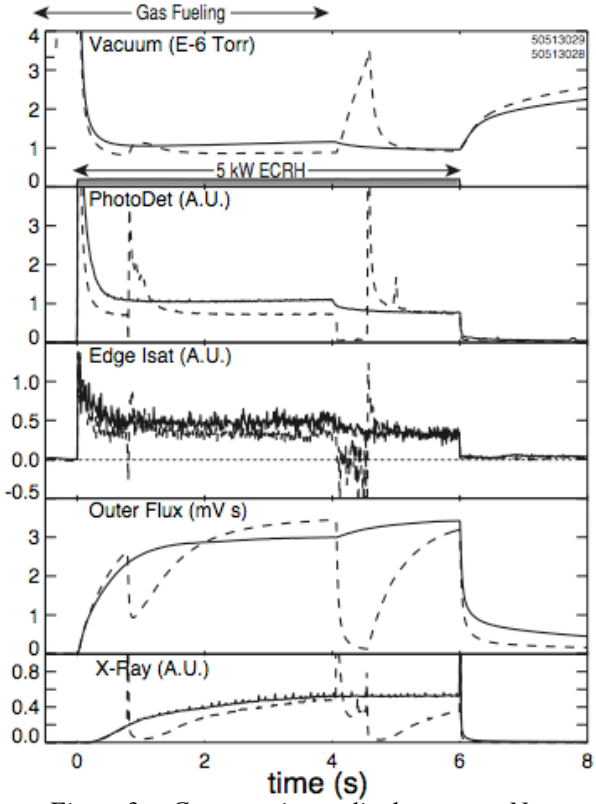

Fig. 3 Consecutive discharges, Nos. 50513028 (dotted line) and 50513029 (solid line), in which gas feed is increased by 15%. From top to bottom, the measurements are (a) vacuum pressure, (b) visible light intensity proportional to plasma line density, (c) edge ion saturation current, (d) plasma diamagnetic flux, and (e) x-rays intensity.

Hot Electron Stability

The observations of stable high-beta electron plasmas confined by axisymmetric mirrors are noteworthy because these plasmas are subject to a high frequency instability driven by the hot electron species and a low frequency mode that feeds on the background plasma and the stability of both of these modes is determined by plasma compressibility. Instability of the high frequency mode requires $\delta(n_{eh}V) < 0$ with n_{eh} the hot electron density [11]. The relation of p_b and n_{eh} to V represents the stabilizing effect of plasma compressibility (which was not significant in previous [12-14] "long-thin" mirror devices). Stability of the high frequency hot electron interchange mode (HEI) has been shown to derive from a stabilizing ion polarization current [15,16] that imposes an instability threshold inversely proportional to the ratio of the line-averaged fast electron and ion densities, n_{eh}/n_i. Thus HEI stability requires sufficient background plasma density and therefore stability of the background plasma (in addition to the condition $\delta(n_{eh}V) < 0$). Recent studies of HEI instability

were performed in low-beta plasma, β < 1%, containing energetic electrons trapped in a supported dipole experiment [17-19]. In the low-beta dipole experiment, the HEI appeared with low azimuthal mode number, m ~1, a broad radial mode structure, and a complex, time-evolving frequency spectrum [19]. Intense bursts of instability induced chaotic radial transport [18] and nonlinear frequency-sweeping was evidence for the inward propagation of ``phase-space holes'' [20].

The transition to and from the high beta regime warrants discussion. In Fig. 3 two consecutive discharges are shown in which the gas fueling is increased by 15% for the second shot, 50513029, as compared with the previous one. When the neutral fueling was lower, in discharge 50513028, the high-beta plasma does not remain stable as indicated by the rapid reductions of the diamagnetic flux observed at t = 0.8 s and at t = 4 s. The first event causes approximately half of the trapped electrons to be lost, and the second event results in nearly complete loss of fast electron confinement. The unstable losses of trapped energetic electrons occur when the neutral gas pressure falls below a critical value, ~1 μTorr. The loss events are accompanied by negative current to the edge probe, by bright x-ray flashes indicating inward fast electron transport, and by rapid decrease in plasma density. When the neutral pressure in the chamber decreases sufficiently, an intense burst of HEI instability initiates at t =0.791 s. The first 1ms of the growing instability appears with broad spectral content (0.2< ω/2π < 6 MHz) that resonate with fast electrons having a wide range of energies that extend beyond 200 keV. During this interval, a large flux of energetic electrons are detected with a negatively-biased edge probe. At t = 0.792 s, the amplitude of the HEI instability saturates and coherent nonlinear frequency sweeping occurs that is associated with bright light and x-ray emission indicating fast electron impact with the dipole. The frequency spectrum, induced fast electron transport, and azimuthal mode structure of these fluctuations resemble previous observations of the HEI instability in a dipole [18, 19].

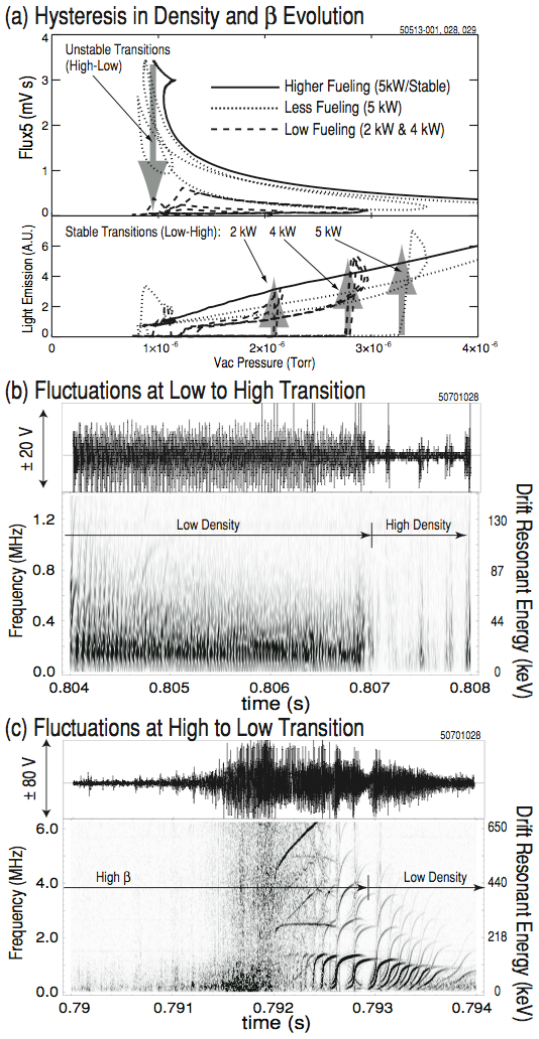

Fig. 4 Hysteresis (a) in the transitions between high beta and low-density operation caused by HEI instability (b,c). In (a), the evolution of three discharges are shown: one, with higher fueling, is always stable; two, with less fueling, have transitions to stability (at 2-3 μTorr) and un-stable HEI transitions to low β (at 1

The transition to and from the high beta state warrants special mention. High neutral fueling is required to create a high beta plasma, but, once stabilized, lower neutral fueling is needed to maintain the high beta state. .Figure 4 shows measurements of the HEI instability at the transitions from low beta to high beta and from high beta to low beta. The frequency spectrum and mode structure of these fluctuations resemble previous observations of HEI in a dipole [18,19]. The radial transport induced by the instability creates hysteresis in the neutral gas

fueling required to maintain sufficient density to stabilize high beta plasma. When the neutral pressure in the chamber is less than a threshold then the HEI instability causes nearly continuous bursts of electrostatic fluctuations as measured with high-impedance floating potential probes (Fig. 3b). Rapid outward transport of fast electrons is observed with negatively-biased edge probes, and inward transport is observed by the target x-rays emitted as electrons impact the dipole. Once the pressure threshold is exceeded, the plasma density and visible light abruptly increases and the HEI immediately stabilizes. As shown in Fig. 4a, this pressure threshold depends upon the ECRH power level. At 2 kW, the HEI is stabilized and the transition to high beta occurs at a pressure just above 2 μTorr. At 4 kW and 5 kW, the transition pressures are 2.8 and 3.2 μTorr. Once the plasma enters the higher density, high beta state, the high-beta electrons remain grossly stable so long as the neutral pressure remains above 1μTorr. When the pressure drops below the threshold (Fig. 4c), the fast electron confinement is destroyed and the plasma density and beta essentially disappear within a few msec. At high beta, the HEI fluctuations can resonate with the drift motion of electrons with high energies E_h > 100 keV; whereas, at low beta, the fluctuations resonate with lower-energy electrons, E_h < 60 keV.

4. Stability of the Background Plasma

The low frequency mode closely resembles the ideal MHD mode and becomes unstable when $\delta(P_b V')$ <0 [10] with P_b the pressure in the background plasma. The background plasma in LDX has n_e ~ 2-5x10^{17} m^{-3} and T_e ~ 10-60 eV, and we observe fluctuations in the diamagnetic drift frequency range (1-10 kHz) and sometimes also in the MHD frequency range (30-100 kHz) that are effected by the rate of neutral fueling and by changes in the plasma size and shape. Both effects presumably change $\eta = d\ln(T)/d\ln(n)$. Furthermore, turbulent fluctuations with an inverse power-law frequency spectrum are observed with optical and probe diagnostics. These low-frequency fluctuations co-exist with the high-beta fast electrons but are most probably associated with convective and/or drift-wave-like modes of the cooler background plasma [12].

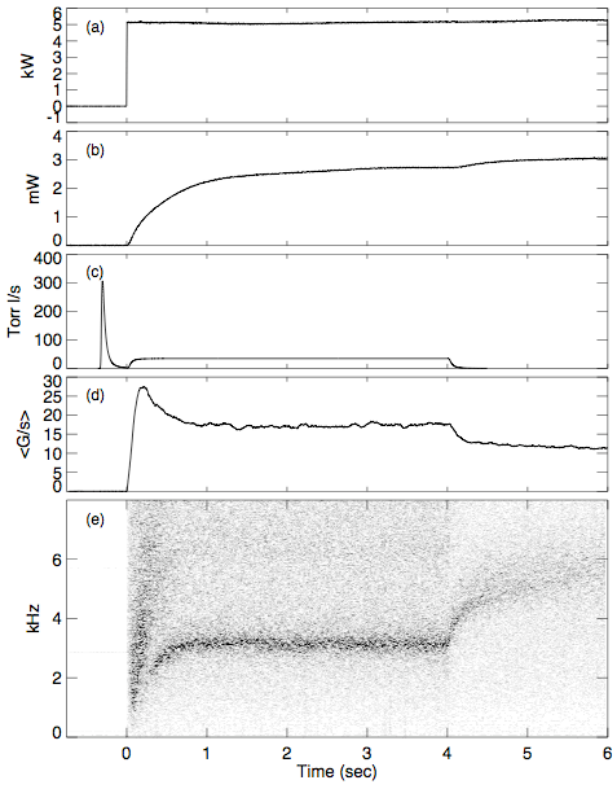

Fig 5. Traces for discharges 50513031 showing respectively a) ECRF heating power, b) plasma diamagnetism, c) puff rate, and d) "Mirnov" magnetic fluctuation signal, e) time frequency domain plot for this discharge.

Figure 5 indicates a discharge with low neutral fueling (p_0<1 μtorr) and with the magnetic geometry as shown in Fig. 1. As in typical discharges 2.5 kW of ECRH power was applied to the plasma at 2.45 and 6.4 GHz (Fig. 5a) which is resonant on the outer midplane 20 cm and 5 cm

respectively from the floating coil. Sufficient neutral gas pressure assures that the plasma enters the high beta regime [1] characterized by a buildup of plasma diamagnetism (Fig 5b), drop in fueling rate (Fig. 5c), and a steady state density profile. Fig. 5d shows the Mirnov coil signal obtained from a coil located just inside of the vacuum chamber wall at the midplane. The time-frequency-domain (TFD) plot for this signal (derived from Fourier analysis with a sliding time window) is shown in Fig. 5e. A similar TFD spectrum is seen on an edge probe, and on a photodiode detector located on the outer plasma midplane. For t<6 s we observe a mode whose frequency rises to f~3.2 KHz. Gas fueling was disabled at t=4 s, at which time the base pressure was $4x10^{-7}$ torr and thereafter the background pressure drops about 10%. The mode frequency was observed to rise abruptly after t=4 s.

Density measurements obtained at a later run [29] with a multi-cord interferometer with cords that are tangent to flux tubes at major radii of 0.77 m, 0.96 m respectively indicate that, after the gas fueling turns off the inner-most cord at (R=0.77 m) is seen to rise while the cord at R=0.96 m falls[29]. This measurement implies a steepening of the profile and indicates that the reduction of neutral pressure is accompanied by a change in the source profile and possibly the existence of a “pinch". Measurements taken at this run also include an array of Mirnov coils placed at 45 deg intervals on the midplane [29] has been analyzed using the “fixed probe pair" analysis [30]. They indicates a toroidal mode number of *m*=1 [29]. Additionally the mode is seen to propagate in the electron diamagnetic direction.

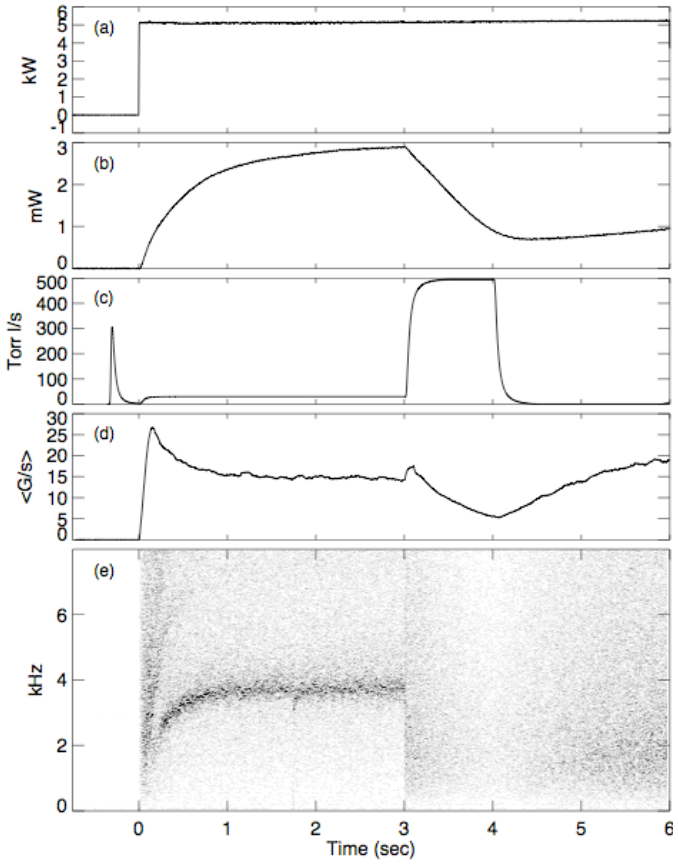

Fig 6. Traces for discharges 50513037 showing respectively a) ECRF heating power, b) plasma diamagnetism, c) puff rate and d) "Mirnov" magnetic fluctuation signal, e) time frequency domain plot for this discharge.

In a second experiment, a one second gas puff was introduced into a similar discharge. At t=3 s a strong 1s gas puff is applied (Fig.6c). Thereafter the density rises within 20 ms and the turbulence turns off. The Mirnov signal (Fig. 6d) indicates a sharp drop in the fluctuation level and the associated TFD plot (Fig. 6e) indicates that this reduction of turbulence extends across the entire range of frequencies (below 10 kHz). A gradual reformation of turbulence is observed after the puff ends at t=4 s. Measurements indicate [29] that strong gas puffing will flatten the density gradient and increase the profile parameter $\eta=d\ln T_{eb}/d\ln n_e$ (which appears in drift wave theory). The gas puff turns off at t=4 s and the profile is seen to again steepen indicating a possible pinch.

6. Conclusions

We report the first production of high beta plasma confined by a laboratory superconducting dipole and demonstrate steady equilibrium for longer than 10 seconds using neutral gas fueling and electron cyclotron resonance heating (ECRH). The superconducting dipole was supported by thin supports in the present experiments, and high-beta plasmas with fast electrons were anisotropic. In future experiments the dipole will be magnetically levitated eliminating particle and energy losses to the supports and additional microwave heating sources will double the injected power and the accessible density. We expect levitation to significantly improve confinement, and the balance of heating and fueling sources with cross-field transport will set equilibrium plasma profiles.

[1] J. Kesner, L. Bromberg, D.T. Garnier, M.E. Mauel, IAEA-F1-CN-69-ICP/09 Yokohama, Japan, *Fusion Energy 1998*. (Proc. 17th Int. Conf. Yokohama, IAEA, 1998).
[2] D.T. Garnier, A. K. Hansen, M.E. Mauel, E.E. Ortiz, A.C. Boxer, J. L. Ellsworth, I. Karim, J. Kesner, S. Mahar, and A. Roach Phys Plasma, **13** (2006) 056111.
[3] A. Hasegawa, Comments Plasma Phys. Controlled Fusion, **1**, 147 (1987).
[4] A. Hasegawa, L. Chen, M.E. Mauel, Nucl. Fusion **30**, 2405 (1990).
[5] M.N. Rosenbluth and C.L. Longmire, Ann. Phys. **1**, 120 (1957).
[6] T. Gold, J. Geophys. Res., **64**, 123 (1959).
[7] D.T. Garnier, J. Kesner, and M.E. Mauel, Phys. Plasmas **6**, 3431 (1999).
[8] V.P. Pastukhov and N.V. Chudin, Plasma Physics Reports **27**, 907 (2001).
[9] J. Kesner, L. Bromberg, D. Garnier, A. Hansen, M.E. Mauel, Nucl. Fusion **44**, 193 (2004).
[10] N. Krasheninnikova, P. Catto, Phys. Pl. **12,** (2005) 32101.
[11] J. Kesner, N. Krasheninnikova, P. Catto, M.E. Mauel, Bull APS, **50**, 35 (2005).
[12] R. A. Dandl, A. C. England, W. B. Ard, H. O. Eason, M. C. Becker, and G. M. Hass, Nuc. Fusion, **4**, 344 (1964).
[13] R. A. Dandl, F. W. Baity Jr., K. H. Carpenter, J. A. Cobble, H. O. Eason et al., Nuc. Fusion, Suppl., v **2**, 355 (1979).
[14] B. Quon, R. Dandl, W. DiVergilo, G. Guest, L. Lao et al., Phys. Fluids, **28**, 1503 (1985).
[15] N. Krall, Phys. Fluids **9**, 820 (1966).
[16] H.L. Berk, Phys. Fluids **19**, 1275 (1976).
[17] M.E. Mauel, Journal de Physique, IV **7**, (1997) 307.
[18] H.P. Warren, M.E. Mauel, Phys. Rev. Lett., 74 (1995) 1351; and H.P. Warren and M.E. Mauel, Phys. Plasmas **2**, (1995) 4185.
[19] B. Levitt, D. Mastovsky, and M.E. Mauel, Phys. Plasmas **9**, (2002) 2507.
[20] D. Maslovsky, B. Levitt, and M. E. Mauel, Phys. Rev. Lett., 185001, **90** (2003).
[21] I. A. Daglis, R. M. Thorne, W. Baumjohann, and S. Orsini, Rev. Geophys., **37**, 4 (1997).
[22] S. von Goeler, S. Jones, R. Kaita, S. Bernabei et al., Rev. Sci. Instr., **65**, 1621 (1994).
[23] X. Chen, B.G. Lane, D. Smatlak, R. S. Post, and S. Hokin, Phys. Fluids B, **1** (1989) 615.
[24] D. Batchelor, Nuc. Fusion **21** (1981) 1615.
[25] M. E. Mauel, Phys. Fluids, **27** (1984) 2899.
[26] S.I. Krasheninnikov and P.J. Catto, Phys. Plasmas, **7**, (2000) 626.
[27] A.N. Simakov, R. J. Hastie, and P.J. Catto, Phys. Plasmas, **7**, (2000) 3909.
[28] D.T. Garnier, A. Boxer, J. Ellsworth, A. Hansen, et al. Phys. Plasmas **13** (2006) 056111.
[29] D.T. Garnier, A.K. Hansen, M.E. Mauel, E.E. Ortiz, A.C. Boxer, J.L. Ellsworth, I. Karim, J. Kesner, "Stabilization of Low Frequency Instability in a Dipole Plasma", submitted to Phys. Plasmas (2006).